

Molecular Recognition and Electron Transfer Across a Hydrogen Bonding Interface

Tarek H. Ghaddar, Edward W. Castner, and Stephan S. Isied*

Department of Chemistry, Rutgers
The State University of New Jersey
Piscataway, New Jersey 08854

Received August 23, 1999

Noncovalent interactions are significant in facilitating molecular recognition and charge transfer in many enzymatic redox processes at protein–protein interfaces.^{1,2} The design of guest (**G**) and host (**H**) molecules, which undergo molecular recognition in solution using hydrogen bonding interactions, provides a means of understanding and controlling the nature of these interactions.^{3–10} The role of the hydrogen bonding in the charge transfer processes of these molecular assemblies could simply be a molecular interface for the reaction, or a more active role in assisting a proton coupled electron-transfer reaction.^{11–13} Weak coupling between the charge-transfer sites and the hydrogen-bonding interface is expected to minimize the latter role.

Here we report on a series of transition metal complexes with hydrogen bonding molecular recognition sites capable of forming noncovalent donor acceptor complexes (Scheme 1). We also determine for the first time the dependence of the rate of intramolecular electron transfer on the reaction driving force across a hydrogen bonding interface.

The strength of the **G–H** interaction in this assembly was shown to be due to the strong hydrogen bonding interaction between **G** and **H** especially when the **G** molecule is in the enolate form.⁴ The amide groups of **H** (Scheme 1) in the **G–H** assembly can be modulated by different substituents to influence their binding to the barbituric acid **G** molecules and therefore control the H-bonding interactions.¹⁴

The molecular nature and the strength of the H-bonding associations in the ruthenium and osmium bipyridine derivatives of **H** and **G** molecules (**Ru^{II}G**, **Os^{II}G**, **HRu^{III}**, and **HOs^{III}**) were determined using NMR and steady-state fluorescence titrations ($K_a = (2 \text{ to } 5) \times 10^5 \text{ M}^{-1}$ in CH_2Cl_2). The fluorescence spectra

and lifetime of **Ru^{II}G** and **Os^{II}G** are similar to those of known [**Ru^{II}(bpy)₃**] and [**Os^{II}(bpy)₃**].¹⁵

Electron-transfer reactions from the excited states of the ***M^{II}G** to **H–M^{III}** in CH_2Cl_2 were determined by fluorescence lifetime measurements (Table 1). The electron-transfer reaction was initiated by laser excitation at $\lambda = 480$ or 400 nm and monitored by observing the quenching of the excited-state emission at $\lambda = 610$ or 710 nm for the different ***M^{II}G–H–M^{III}** complexes. All **M^{II}G–H–M^{III}** complexes show biphasic emission decay with short lifetimes corresponding to the intramolecular electron transfer within ***M^{II}G–H–M^{III}** ($\tau = 4\text{--}7$ nsec) and longer lifetimes corresponding to the emission of the uncomplexed ***M^{II}G** ($M = \text{Ru}$, $\tau' = 770$ ns; $M = \text{Os}$, $\tau' = 90$ ns). Carrying out the experiments in 3:1 ethanol–methylenechloride resulted in the disruption of the H-bonding association and the disappearance of the fast component ($\tau = 4\text{--}7$ ns). The thermal back electron-transfer reaction in CH_2Cl_2 from **H–M^{II}** to [**M^{III}G**] was determined by transient absorption techniques. The [**M^{III}G–H–M^{II}**] intermediate was generated from the excitation of **M^{II}G–H–M^{II}** (generating ***M^{II}G–H–M^{II}** as the long-lived excited state) which is then quenched by 1,4-benzoquinone.¹⁶ Changes in absorption of the intermediate (Figure 1) were monitored between 450 and 550 nm. No transient absorption for **H–M^{II}** was observed in 3:1 ethanol–methylenechloride, with benzoquinone, confirming the absence of the H-bonding association.

The forward and reverse electron-transfer reaction rates of the **M^{III}G–H–M^{III}** complexes were plotted against their respective free energies (Figure 2). Analysis of the experimental points for both the forward and back electron-transfer reactions using the classical Marcus equation¹⁷ (without assuming a known λ_{el}) results in $\lambda_{\text{el}} \sim 1.2$ eV and $H_{\text{ad}} = 1.2$ cm⁻¹. Alternatively, the forward electron-transfer reaction rates were analyzed after estimating the reorganization energy for the reaction $\lambda_{\text{el}} \sim 1.0$ eV.¹⁸ From this analysis, H_{ad} was calculated to be 1.7 cm⁻¹. The same analysis for the thermal back electron-transfer reaction gave $\lambda_{\text{el}} \sim 0.9$ eV¹⁸ and $H_{\text{da}} = 0.4$ cm⁻¹. Both analyses are offered here because our data cannot distinguish between these similar values. Comparison of the electron transfer rates determined here to those in related, but covalently bonded complexes¹⁹ shows that, at similar distances, electron transfer rates across H-bonding interfaces are only modestly slower than that observed in the covalently bonded donor–acceptor complexes.

The work presented here demonstrated how the driving force dependence of the rates of intramolecular electron transfer reactions in these H-bonded complexes can be used to determine the electronic coupling matrix element for electron transfer. Comparison of these H-bonded systems with similar covalently bound complexes at similar distances¹⁹ shows that a H-bonding interface can be as effective a bridge for electron transfer as covalently bound bridges.^{8–9,11–13} The advantage of the donor–

*To whom correspondence should be addressed. e-mail: isied@rutchem.rutgers.edu.

- (1) Pelletier, H.; Kraut, J. *Science* **1992**, *258*, 1748.
- (2) Nocek, J. M.; Zhou, J. S.; DeForest, S.; Priyadarshy, S.; Beratan, D. N.; Onuchic, J. N.; Hoffman, B. M. *Chem. Rev.* **1996**, *96*, 2459.
- (3) Lawrence, D. S.; Jiang, T.; Levett, M. *Chem. Rev.* **1995**, *95*, 2229.
- (4) Chin, T.; Gao, Z.; Lelouche, I.; Shin, Y. K.; Purandare, A.; Knapp, S.; Isied, S. S. *J. Am. Chem. Soc.* **1997**, *119*, 12849–12858.
- (5) Tecilla, P.; Dixon, R. P.; Slobodkin, G.; Alavi, D. S.; Waldeck, D. H.; Hamilton, A. D. *J. Am. Chem. Soc.* **1990**, *112*, 9408–9410.
- (6) (a) Sessler, J. L.; Wang, B.; Harriman, A. *J. Am. Chem. Soc.* **1995**, *117*, 704–714. (b) Sessler, J. L.; Brown, C. T.; Wang, R.; Hirose, T. *Inorg. Chim. Acta* **1996**, *251*, 135–140. (c) Harriman, A.; Kubo, Y.; Sessler, J. L. *J. Am. Chem. Soc.* **1992**, *114*, 388–390. (d) Harriman, A.; Magda, D. J.; Sessler, J. L. *J. Phys. Chem.* **1991**, *95*, 1530–1532. (e) Harriman, A.; Magda, D. J.; Sessler, J. L. *J. Chem. Soc., Chem Commun.* **1991**, 345–348.
- (7) Armaroli, N.; Barigelletti, F.; Calogero, G.; Flamigni, L.; White, C. M.; Ward, M. *Chem. Commun.* **1997**, 2181–2182.
- (8) Osuka, A.; Yoneshima, R.; Shiratori, H.; Okada, T.; Taniguchi, S.; Mataga, N. *Chem. Commun.* **1998**, 1567–1568.
- (9) Yang, J.; Seneviratne, D.; Arbatin, G.; Andersson, A. M.; Curtis, J. C. *J. Am. Chem. Soc.* **1997**, *119*, 5329–5336.
- (10) Cusack, L.; Rao, S. N.; Fitzmaurice, D. *Chem. Eur. J.* **1997**, *3*, 202–207.
- (11) (a) Cukier, R. I.; Nocera, D. G. *Annu. Rev. Chem.* **1998**, *49*, 337–369. (b) Kirby, J. P.; Roberts, J. A.; Nocera, D. G. *J. Am. Chem. Soc.* **1997**, *119*, 9230–9236.
- (12) de Rege, P. J. F.; Williams, S. A.; Therien, M. J. *Science* **1995**, *269*, 1409–1413.
- (13) For theoretical approach see: Baratan, D. N.; Betts, J. N.; Onuchic, J. N. *Science* **1991**, *252*, 1285.
- (14) Salameh, A.; Ghaddar, T.; Isied, S. S. *J. Phys. Org. Chem.* **1999**, *12*, 247–254.

(15) (a) Balzani, V.; Juris, A.; Venturi, M. *Chem. Rev.* **1996**, *96*, 759–833. (b) Kober, E. M.; Caspar, J. V.; Sullivan, B. P.; Meyer, T. J. *Inorg. Chem.* **1988**, *27*, 4587–4598.

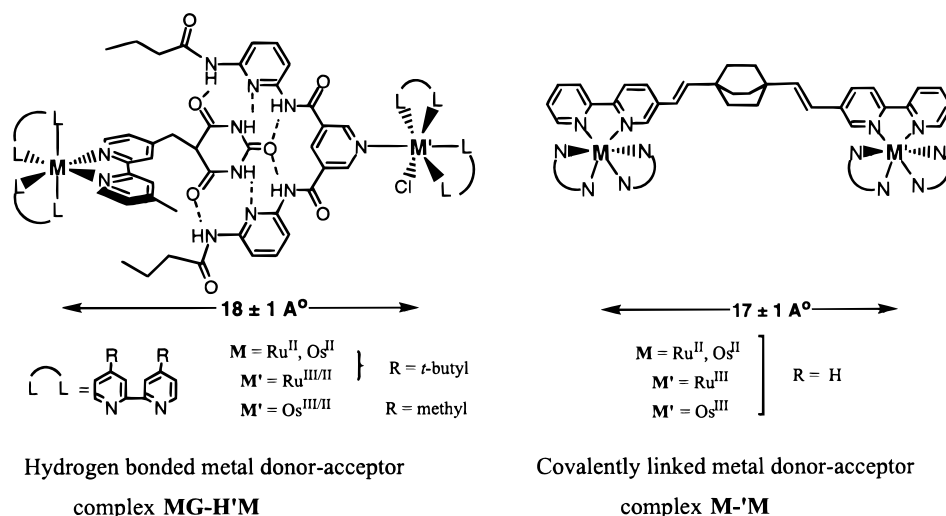
(16) The experiment was done using 0.1 M benzoquinone and 0.1 M tetrabutylammonium hexafluorophosphate in methylenechloride. The rate constant of quenching of **Ru^{II}G** with 1,4-dibenzoquinone was measured to be $4.1 \pm 0.5 \times 10^9 \text{ M}^{-1} \text{ s}^{-1}$. The rate constant of oxidative quenching between ***Ru(bpy)₃²⁺** and 1,4-dibenzoquinone in acetonitrile at 298 K is reported to be $1.1 \times 10^{10} \text{ M}^{-1} \text{ s}^{-1}$; Kim, H.-B.; Kitamura, N.; Kawanishi, Y.; Tazuke, S. *J. Phys. Chem.* **1989**, *93*, 5757–5764.

(17) Marcus, R. A.; Sutin, N. *Biochim. Biophys. Acta* **1985**, *811*, 265.

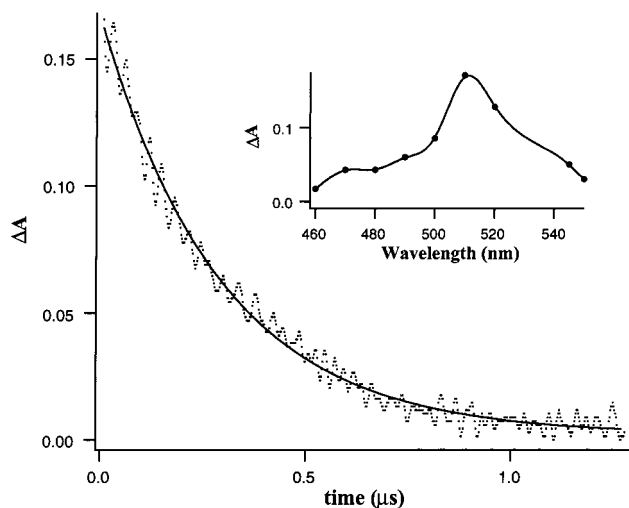
(18) The reorganization energy $\lambda_{\text{el}} = \lambda_{\text{in}} + \lambda_{\text{out}}$ was calculated using $\lambda_{\text{in}} = 0$ eV for the back electron-transfer reactions and 0.1 eV for the forward ones. λ_{out} was calculated using the following equation: $\lambda_{\text{out}} = e^2(1/m^2 - 1/\epsilon_s)(1/2r_a + 1/2r_b + 1/r_{\text{ab}})$. For methylene chloride $n = 1.4244$ and $\epsilon_s = 9.08$. For the metal complexes, $r_a = r_b \sim 4.3$ Å and $r_{\text{ab}} \sim 18$ Å; Sutin N. *Acc. Chem. Res.* **1982**, *15*, 275–282.

(19) De Cola, L.; Balzano, V.; Barigelletti, F.; Flamigni, L.; Belsler, P.; von Zelewsky, A.; Frank, M.; Vogtle, F. *Inorg. Chem.* **1993**, *32*, 5228–5238.

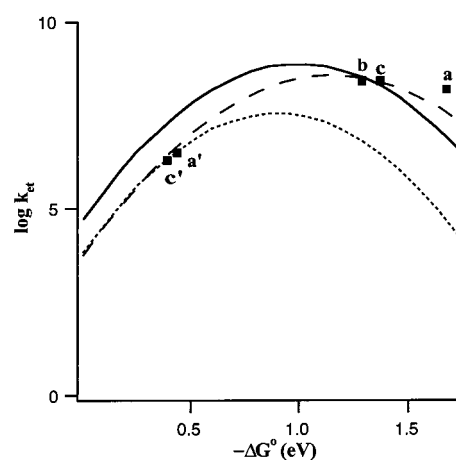
Scheme 1

**Table 1.** Experimental Binding Constants, Electron Transfer Rates, and Related Parameters

complex	K_a (M^{-1})	k_{et} , s^{-1}	ΔG° , eV
* $Ru^{II}G-HRu^{III} \rightarrow Ru^{III}G-HRu^{II}$	$(3 \pm 1) \times 10^5$	1.5×10^8	-1.68
* $Ru^{II}G-HOs^{III} \rightarrow Ru^{III}G-HOs^{II}$	$(2 \pm 1) \times 10^5$	2.5×10^8	-1.29
* $Os^{II}Gst-HOs^{III} \rightarrow Os^{III}G-HOs^{II}$	$(5 \pm 1) \times 10^5$	2.6×10^8	-1.37
$[Ru^{III}G-HRu^{II}] \rightarrow Ru^{II}G-HRu^{III}$		3.3×10^6	-0.44
$[Os^{III}G-HOs^{II}] \rightarrow Os^{II}G-HOs^{III}$		2.0×10^6	-0.39

**Figure 1.** The fitted decay of HRu^{II} transient absorption in the electron-transfer reaction of $[Ru^{III}G-HRu^{II}]$. The spectrum of the transient absorption of HRu^{II} is shown in the insert.

acceptor assembly studied here is the ability to systematically introduce substituents on the host **H** molecule which results in varying the strength of the H-bonding association by electronic and steric means.¹⁴ This may enable one to obtain more detailed measurements of the electron-transfer processes *across the same molecular interface* in different solvents. In addition to this, the deuterium isotope effect on the binding and the electron-transfer process may provide new insights and answers to the question of the direct involvement of the hydrogen bond in the charge-transfer process or its indirect role in holding the reactants close enough for direct overlap.

**Figure 2.** A plot of $\log k_{et}$ vs driving force for the electron-transfer reactions of the different host-guest molecules. a, b, and c indicate the forward electron-transfer reactions for * $Ru^{II}G-HRu^{III}$, * $Ru^{II}G-HOs^{III}$, and * $Os^{II}G-HOs^{III}$, respectively. a' and c' indicate the back electron-transfer reactions for $[Ru^{III}G-HRu^{II}]$ and $[Os^{III}G-HOs^{II}]$. The dashed line is a fit for the back and forward electron-transfer reactions. The solid and dotted lines are fits to the forward and back electron-transfer reactions, respectively.

Acknowledgment. This work was supported by the U.S. Department of Energy, Division of Chemical Sciences, Office of Basic Energy Sciences under contract DE-FG05-90ER1410. The work at Brookhaven National Lab is supported by contract DE-AC-02-98CH10884. The authors would like to thank Professor F. Long and R. Ebricht (Rutgers) and Dr James Wishart (Brookhaven) for the use of their laser systems and Dr. Bruce Brunshwig (Brookhaven) for helpful discussions.

Supporting Information Available: Synthesis of the different metal complexes and their electrochemical and spectroscopic data, luminescence data of $Ru^{II}G$ and $Os^{II}G$ at 77 and 298 K in methylenechloride and butyronitrile, luminescence decay of $Ru^{II}G-Os^{III}H$ in methylenechloride and ethanol-methylenechloride, fluorescence titration of $Ru^{II}G$ and HRu^{III} in methylenechloride, and the fit to obtain the binding constant (PDF) are available. This material is available free of charge via the Internet at <http://pubs.acs.org>.